

Quark confinement and white-black hole duality: Part 1: Gauge symmetry breaking in 4D fractional quantum Hall superfluidic space-time

A. E. Inopin*

*Department of Experimental Nuclear Physics,
Karazin National University,
Svobody Sq. 4,
Kharkiv, 61077, Ukraine*

N. O. Schmidt†

*Department of Mathematics,
Boise State University,
1910 University Drive,
Boise, Idaho, 83725, USA
(Dated: September 24, 2012)*

In this first paper of the series, we demonstrate that quarks and antiquarks are confined to baryons and antibaryons, respectively; we prove color-anticolor confinement for a baryon-antibaryon pair in an upgraded Gribov vacuum. We identify the core topologies, dualities, fractional statistics, quantum number order parameters, and baryon wavefunction antisymmetries in 4D fractional quantum Hall superfluidic space-time, where space and time are dual and conjugate. A White Hole Bag and Black Hole Bag model baryons and antibaryons, respectively; the bags are dual, opposite, inverse, and reverse, and are combined to form a White-Black Hole Bag. The quark-antiquark pairs are confined to the Riemannian holographic ring unit circle of two counter-propagating edge channels with Rashba spin-orbit coupling on the Fermi scale: a Fermi surface and Mott insulator. The three distinct quark-antiquark pairs for a baryon-antibaryon pair are arranged along the antiferromagnetic six-coloring kagome lattice manifold; an $SU(2)$ -gauged Bose-Einstein condensate between two superconductive, superfluidic 3-branes that imposes double-confinement and double-stereographic superlensing on *two* dynamical scales for skyrmions with “massive ‘Higgs-like’ scalar amplitude-excitations” and “massless Nambu-Goldstone pseudo-scalar phase-excitations.” We prove that White-Black Hole Confinement and White-Black Hole Duality are the mechanisms for the superlensing of baryons and antibaryons.

I. INTRODUCTION

Nature presents an impressive display of mass-energy puzzles in physics. Black Holes (BH) are one of the most intriguing objects in nature, both theoretically and experimentally. Being predicted in 1916 by Karl Schwarzschild, until recently there has been no clear experimental evidence of BHs¹. White Holes (WH) are the hypothetical *reverse* of BHs, which were predicted by the theory of general relativity (GR); amazingly, there has been no clear experimental evidence of WHs². Moreover, the apparent asymmetry of matter and antimatter in the visible universe is one of the greatest unsolved problems in physics³. In this series of papers, we chase down these mysteries. *The theory is directly supported by special relativity (SR) and GR, and does not contradict or replace quantum chromo dynamics (QCD) and quantum electro dynamics (QED); it merely “upgrades” the accuracy and precision of QCD and QED so they are consistent with SR and GR.* Mathematical and experimental proof for these claims is provided in this paper.

Quarks and antiquarks are the fundamental building blocks of matter and antimatter, respectively. We prove that baryons are WHs and antibaryons are BHs. The *dual* WH and BH quantum states are encoded with quantum number order parameters of fractional statistics for

quasiparticles. We prove quark-antiquark confinement in terms of Laughlin excitations⁴ that dynamically arise due to our *fractional quantum Hall superfluidic* (FQHS) space-time and topology inspired by the quasiparticle interferometer experiments of Goldman⁵. We prove that the quarks and antiquarks confined to the holographic ring “cancel out” due to the CPT-Theorem. Spontaneous symmetry breaking (SSB) generates massless “Nambu-Goldstone pseudo-scalar *phase-excitations*”^{6–9} and massive “Higgs-like scalar *amplitude-excitations*”¹⁰ of Laughlin statistics⁴

In Section II, we introduce the quark-antiquark confinement, duality, and bag models in FQHS space-time. We explain how WHs and BHs can vary in size, where their duality is evident on the Fermi scale. Moreover, we investigate the two dynamical scales that arise in the double confinement, double stereographic superlensing, and double horizons inherent to WHs and BHs. We prove that a WH-BH pair is composed of three distinct quark-antiquark pairs, which form three corresponding “thin color-electric flux tubes”¹¹ of Laughlin excitations⁴ and fractional statistics¹². We discuss the hadronization process and the modified Gribov vacuum, where all properties in 3D Schwarzschild space can be inferred from the analogue of the 2D gauge field on the six-coloring kagome lattice manifold. Additionally, we venture to the interaction between the boson propagators and gravity

by introducing “*gravitational birefringence*”.

In Section III, we discuss the surface and generalized Riemann coordinates used to encode our FQHS space-time scenario. We extend the definition of complex numbers and use them to represent locations on the 1D Riemann surface; we prove that the complex numbers are both scalars and Euclidean vectors. We define axis constraints for the vectors, which let us construct a powerful 2D generalized coordinate system on the surface equipped with the Pythagorean identity; the locations may always be expressed in terms of right triangles with real and imaginary components.

In Section IV, we explore the three distinct topological sub-surface zones for a WH and BH using set and group theory. We formally define the zones using trichotomy and our generalized coordinates for 2D and 3D space. We prove that the time-like region is a holographic ring—a closed curve and simple contour of points, which can be scaled to, for example, the Fermi radius. We formally define space and time as being dual. Additionally, we demonstrate that the time-like region represents the $U(1)$ and $SU(2)$ symmetry groups, which is isomorphic to the $SO(3)$ orthogonal group; all 3D properties are inferred directly from the 2D holographic ring for the $SU(2)$ gauged Bose-Einstein condensate.

In Section V, we define the White-Black wavefunction (WBWF) of fractional quantum number order parameters (OP) for our quark (q) and antiquark (\bar{q}) confinement proof. Additionally, we discuss the amplitude-excitations¹⁰ and phase-excitations^{6–9} for Laughlin quasiparticles⁴ experienced by the WBWF OPs in our FQHS space-time scenario. For this, we express the full WBWF antisymmetries and CPT-transformations.

In Section VI, we express the Lagrangian in terms of *effective potential* and *effective kinetic* for our FQHS space-time scenario. For this, we apply both Newtonian and Einsteinian concepts to the q and \bar{q} confinement proof and thereby incorporate *effective force*, *effective mass*, and *effective acceleration*.

To summarize, in this first paper of the series we introduce the topologies, vacuum, generalized coordinates, fractional statistics, quantum number OPs, WBWF, gauge symmetry breaking, and Lagrangian for the q and \bar{q} confinement proof in FQHS space-time; for the scenario, we provide a series of colorful depictions and an array of experiments supporting this construction. In the next paper(s) of this series, we will extend our confinement scenario by discussing the anyons, phase locking¹³, Hubius helix (HH)¹⁴, attractive and repulsive gravitational effects of quasiparticle signals on the Lagrangian, modified Gullstrand–Painlevé reference frames, and Magnification Effect.

II. ALIGNMENT TO CONFINEMENT

A BH’s event horizon confinement radius $\epsilon_{BH} = 2M_{BH}$ strongly depends on its mass M_{BH} , which can vary in scale from the elementary or so called quantum-dot, to billions of solar-masses. Regardless of scale, this is known as *Black Hole Confinement* (BHC) and is modeled as a *Black Hole Bag* (BHB). Similarly, a WH’s event horizon confinement radius $\epsilon_{WH} = 2M_{WH}$ strongly depends on its mass M_{WH} , a variable which is well defined in terms of the atomic numbers of the periodic table of elements and stars throughout the universe. This is known as *White Hole Confinement* (WHC) and is modeled as a *White Hole Bag* (WHB). The universe is self-similar. Within this prodigious spectrum there exists the Fermi scale, at which baryon symmetry is perhaps most evident; here, these two seemingly unrelated phenomena merge to reflect quark-antiquark confinement. For example in a proton-antiproton pair, an antiproton of antimass $M_{BH} = M_{antiproton} = 1$ GeV precisely counterbalances a proton of mass $M_{WH} = M_{proton} = 1$ GeV due to antiferromagnetic ordering. On this scale we identify the general mechanism, namely *White-Black Hole Confinement* (WBHC), which is responsible for the dynamics. It is based on the appearance of a critical radius $\epsilon_{2M} = \epsilon_{WH} = \epsilon_{BH}$ for quark-antiquark confinement at the 1 Fermi scale and the appropriate generalized dynamics—effective gravito-strong interaction. So in gravity plus electromagnetism, there is one interesting mechanism—radiation trapping just on the horizon’s surface, that is a coherent particle accumulation structure¹³ of fractional statistics and *toroidal vortex*¹⁵. The toroidal vortex, that stores information as in the holographic hypothesis¹¹, intertwines the WHC and BHC mechanisms, creating WBHC. The toroidal vortex forms between the spherical shells defined at the *inner confinement radius* ϵ_{2M} and the *outer confinement radius* $\epsilon_{3M} = 3M$ (based on the effective potential); ϵ_{2M} and ϵ_{3M} correspond to the “horizon” and “imaginary surface”, respectively, in Figure 6 of Witten¹¹; there are two distinct quantum critical points imposed by a BH or WH for the *double stereographic superlense* with the metamaterial, acoustic, double-negative refractive index, and sub-wavelength features of^{16–19}—see Figure 1. These facts are evident from the DIS modeling results of the hadronization process²⁰. Quark-hadron duality in jet formation in DIS leads to a two-step process of hadronization, with *two scales* appearing: large $Q_0^2 \gg \Lambda_{QCD}^2$ and small $Q_0^2 \sim 1\text{GeV}^2$. An alternative approach in DIS, namely “Local Parton Hadron Duality”, also leads to the *two dynamical scales*: $k_{perp} = Q_0 \sim \Lambda_{QCD}$ and $k_{\perp} = Q_0 \sim 1$ GeV²⁰. Both models of the hadronization process give us the numbers in accord with our model $\epsilon_{2M} \sim 0.2 - 0.3$ fm and $\epsilon_{3M} \sim 1$ fm. Another fresh perspective can be taken from the “Glue drops” model²¹, where the authors gave firm evidence of the existence of a non-perturbative scale, smaller than the usual $\frac{1}{\Lambda_{QCD}} \sim 1$ fm, which is related to gluonic degrees of freedom. The

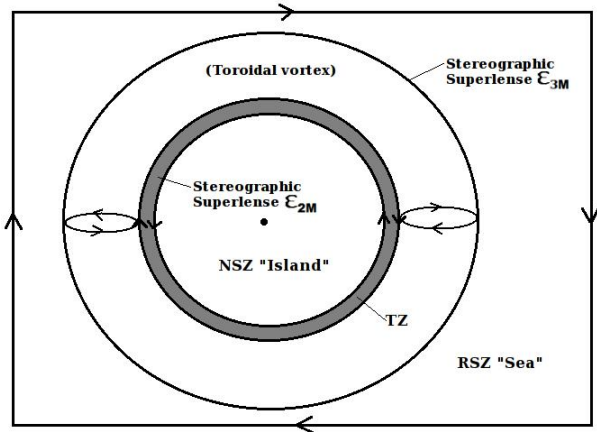


FIG. 1. The Riemannian holographic ring unit circle of two counter-propagating edge channels defines the TZ for quark-antiquark confinement and is isometrically embedded on the 1D Riemann surface. The toroidal vortex between two dynamical scales for a double stereographic superlens: the spherical shells located at critical radius $\epsilon_{2M} = 2M$ and $\epsilon_{3M} = 3M$.

evidence for the presence of a *semi-hard* scale in hadronic structure is reviewed from many venues. The most notable effects are: QCD sum rules gives 0.3 fm radius of the corresponding form factor, lattice gives 0.2-0.3 fm for the correlation length, instanton radius peaks approximately at 0.3 fm, diffractive gluon bremsstrahlung in hadronic collisions leads to k_{\perp} for the gluons in a proton of about 0.7 GeV²². At higher scales, chiral symmetry breaking is restored and the vacuum does not feel apparent existence of quark and gluon condensates, which spoil the chiral symmetry from the start—the mechanism for the *spontaneous breaking of chiral symmetry* and *spontaneously emergent behavior* of chaos theory on the Lagrangian.

All together, this brings us to the concept of *White-Black Hole Duality* (WBHD), which is responsible for the stereographic superlensing¹⁸ dynamics. At rest, the massless red, green, and blue quarks are confined to a WH and circulate *counter-clockwise* along it's event horizon as a *left-handed* HH (WHH)¹⁴ at the speed of light to generate *effective mass*, such that all observable baryons are *white*; the *visible* colored quarks are *non-Abelian color-electric-magnetic monopoles*²³ which emit red, green, and blue light-rays to render a WH. Similarly, the resting antired, antigreen, and antiblue antiquarks are confined to a BH and circulate *clockwise* along it's event horizon as a *right-handed* HH (BHH)¹⁴ to generate *effective antimass*, such that all “observable” antibaryons are *black*; the “visible” anticolored antiquarks are *non-Abelian anticolor-electric-magnetic antimonopoles*²³ which emit antired, antigreen, and antiblue light-rays to render a BH; the relative direction of circulation (with corresponding winding number) distinguishes between mass (i.e. M_{proton}) and antimass (i.e. $M_{antiproton}$). For WBHD, the WH and BH bags are dual, opposite, reverse, and inverse, and are there-

fore modeled as a *White-Black Hole Bag* (WBHB). The quark and antiquark trajectories follow Wilson loops and form a self-consistent⁶ $SU(2)$ gauged Bose-Einstein condensate²⁴. These so-called screened quark-gluon potentials are again dual to the BH radiation mechanisms by Hawking. The electro-strong duality of the potentials continuously transform in FQHS space-time in accordance with 1D, 2D, and 3D skyrmions²⁴.

This rich concept of duality enables us to compute observables in time-like regions, given the physics in space-like regions, and vice-versa. Upon considering these dual fields, the idea of *two distance scales* comes up naturally. Our 1D Riemann surface (2D holographic information structure) is divided into three distinct topological sub-surfaces for quasiparticles:

1. *Non-Relativistic Space Zone* (NSZ) or “Micro” distance scale of *superluminal* signals,
2. *Time Zone* (TZ), and
3. *Relativistic Space Zone* (RSZ) or “Macro” distance scale of *luminal* signals.

The Riemannian holographic ring unit circle represents the TZ and is isometrically embedded on the surface; it bifurcates 3D space to establish the NSZ, such that $0 < x < \epsilon_{2M}$, and the RSZ, where $\epsilon_{2M} < x < \infty$ —recall Figure 1. The gauge field is a 3D analogue of the TZ's Rashba spin-orbit coupling²⁴—see Figure 4. The quarks (and leptons) are “split” into three distinct excitation degrees of freedom, namely spinon, holon, and orbitons^{4,25}; the Laughlin excitations of the FQHS 3-branes obey fractional statistics; luminal quasiparticle signals of the RSZ “sea” execute a closed path around the NSZ “island” of superluminal quasiparticle signals and thus acquire statistical phase⁵—see Figure 5.

In QCD, WBHC is a difficult strong coupling problem, but a somewhat similar phenomenon in nature is much better understood in QED. The Meissner effect is the fundamental observation that a superconductor expels magnetic flux. Suppose that magnetic monopoles become available for study and that we insert a monopole-antimonopole pair into a superconductor, where the two poles are separated by a large distance x . What will happen? A monopole is inescapably a source of the magnetic flux, but magnetic flux is expelled from a superconductor. So the optimal solution to this problem, energetically, is that a thin, *non-superconducting* tube forms between the monopole and the antimonopole. The magnetic flux is confined to this region, which is known as an *Abrikosov-Gorkov* flux tube (or a *Nielsen-Olesen* flux tube in the context of relativistic field theory). The flux tube has a certain nonzero energy per unit length, so the energy required to separate the monopole and antimonopole by a distance x grows linearly in x , for large x .

As a non-Abelian gauge theory, QCD has fields rather similar to ordinary electric and magnetic fields but obey a *nonlinear* version of Maxwell's equations. Quarks and antiquarks are particles that carry the QCD analog of

electric charge and are confined in to our QCD vacuum just as ordinary magnetic charges would be in a superconductor. The color-electric-magnetic quark monopoles and anticolor-electric-magnetic antiquark antimonopoles may be separated by a large distance x to form non-Abelian dipoles: red-antired, green-antigreen, and blue-antiblue “thin color-electric flux tubes”¹¹. Now from the Aharonov–Casher (AC) effect and Aharonov–Bohm (AB) effect duality^{26–28}, it is evident that this analogy immediately leads to the idea that *the QCD vacuum is to a superconductor, just as electricity is to magnetism, and just as the AC effect is to the AB effect*—see Figure 3.

Furthermore, analogy between WH and BH physics revealed itself again recently in Olsson’s model²⁹. The author considered a relativistic string model, where a massless quark moves at the speed-of-light in a circular orbit. One can see clearly the $x = x_0 = \epsilon_{2M}$ coordinate represents an event horizon or “impenetrable barrier” and the quark moves in the “half harmonic oscillator” potential. When combined with the phenomenological aspects of^{30,31}, a strong QCD/QED string model for the $q\bar{q}$ pairs with the associated quasiparticles⁴ emerges in our scenario. So for the $q\bar{q}$ pairs we identify both open-ended (“linear”) fermionic strings *and* the closed (“non-linear”/circular) bosonic strings vibrating in our conjugate and dual space-time. All of this is supported by Glue drops²¹, where the energy of a QCD string is concentrated in a thin color-electric flux tube¹¹ of radius $\epsilon_{2M} = 0.3$ fm. All such particles and quasiparticles on the Riemann surface which generate effective mass (and antimass) are projected along the “ z -axis” to effective 3D space (recall Figure 4). Here, events are represented on the Lagrangian using generalized coordinates in Schwarzschild space-time on the Riemann surface.

Viewed in certain classes of inertial frames, a superluminal signal travels *backwards* in time. In QED, Feynman diagrams involve a virtual e^+e^- pair that influences the photon propagator. Here, positrons are replaced with electron-holes. This gives a photon an effective mass (or antimass) on the order of the Compton wavelength for the electron (or electron-hole); leptons are split into quasiparticles^{4,25}. All of this is generalized to QCD, where a virtual $q\bar{q}$ pair influences the gauge boson propagator in FQHS space-time; the propagator is a function which returns a probability amplitude of 1 for the quarks and baryon confined to the TZ. In both QED and QCD, if the space-time curvature has a comparable scale, then an effective boson-gravity interaction is induced; the Higgs-like amplitude excitations¹⁰ for the WH-BH pair impose effective mass for WHs and quarks, and effective antimass for BHs and antiquarks. This depends explicitly on the curvature, in violation of the Strong Equivalence Principle. The boson velocity is changed and light-ray no longer follows the shortest possible path—it bifurcates to both the NSZ and RSZ distance scales. Moreover, if the space-time is anisotropic, this change can depend on the boson’s polarization as well as direction. This is the quantum phenomena of “gravitational birefringence”.

The effective light-cones for boson propagation in gravitational fields *no longer coincide* with the geometrical light-cones fixed by the local Lorentz invariance of space-time, but depend *explicitly* on the local curvature. This formulation agrees with the von Karman flow and symmetry breaking of³², the kaleidoscope of exotic quantum phases in the 2D frustrated model of³³, and the deviant Fermi liquid of³⁴, where the TZ serves a Bose metal as in³⁵. All this works in 4D space-time.

The $q\bar{q}$ pairs for a WH-BH pair are “superbound” to the vacuum³⁶ as coupled oscillators³⁷ (see Figure 2) and form red-antired, green-antigreen, and blue-antiblue *Nambu-Goldstone pions*, which are Nambu-Goldstone bosons; the SSB of the three distinct pions generates colored amplitude-excitations¹⁰ and phase-excitations^{6–9}. The $q\bar{q}$ pairs of the three distinct thin color-electric flux tubes are confined to the TZ, which is a *Riemannian holographic ring unit circle* on a 1D Riemann surface equipped with a six-coloring (three coloring plus three anticoloring) kagome lattice manifold generalization of³⁸ with antiferromagnetic ordering⁴. The ring exhibits the Rashba and fractional quantum Hall effects³⁹, along with spin-Hall current⁴⁰ and chiral magnetic moments⁴¹. The $q\bar{q}$ pairs are uniformly arranged along the kagome lattice with the triangular chirality of⁴² and the self-assembling observables of^{13,43} (recall Figure 3). The quasiparticles of the $SU(2)$ gauged Bose-Einstein condensate are direct 3D analogs of the spontaneously emerging QED and QCD. The kagome lattice hexagonal structure is self-similar to, for example, graphene, which explains the “plasmaron” observations in quasi-freestanding doped graphene⁴⁴ and the “soundaron” observations of⁴⁵. The quarks can also be thought as moving along the “caustics” inside the toroidal vortex, where the quark’s trajectories are trapped between the dual scale dynamics—they are “gliding” along the surface and are reflected back to the center. The dual confinement boundaries located at ϵ_{2M} and ϵ_{3M} act as reflecting and focusing stereographic superlenses. So WHs and BHs become *seashells* closed on ϵ_{3M} ⁴⁶.

When we come to the vacuum estate, the richness of WBHD is shining brightly: Gribov’s QED/QCD vacuum³⁶ resembles a complicated structure of *Unruh-Boulware-Hartle-Hawking’s* BH vacuum and is fed with solid-state physics along with notions of forbidden zones, Fermi surfaces, particles and holes to encode the WBHB on the Riemann surface. But there are some new diagrams that arise with the new zones, and novel types of excitations—enabling us to upgrade Gribov’s model. This new vacuum differs drastically from Dirac’s vacuum and contains a total of 18 zones for the six-coloring (kagome lattice) manifold on the Riemann surface—Figure 4; these zones are populated with quasiparticles^{4,25} spontaneously generated by the $q\bar{q}$ pairs confined to the TZ with the spin-orbit coupling of^{40,49–51}. The TZ acquires a geometric phase^{26,27,52}, so the quasiparticles confined to the TZ are dual to those signals propagated across the NSZ and RSZ zones.

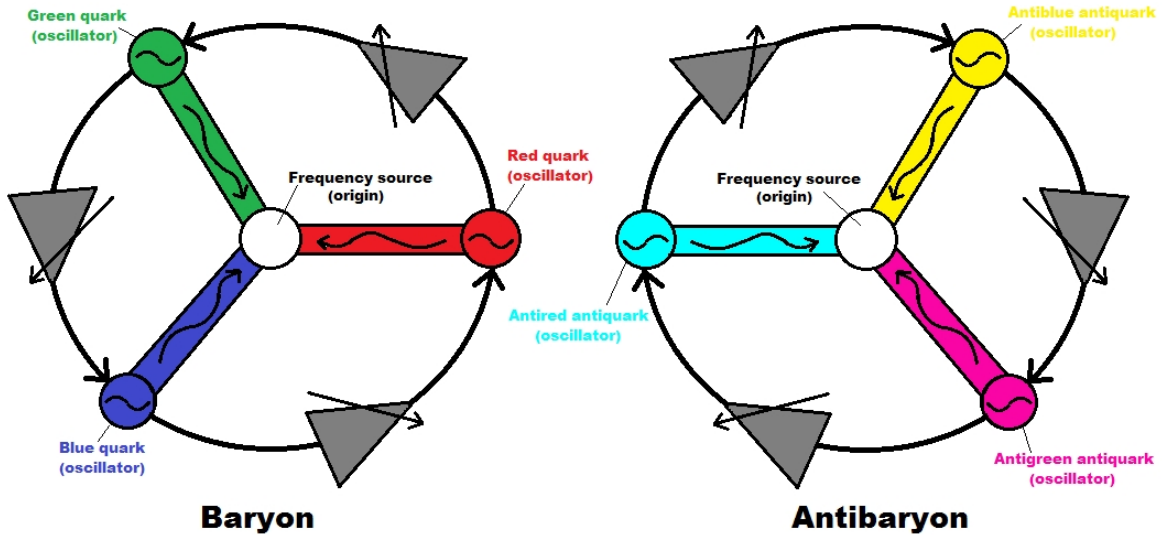


FIG. 2. Schematic of the multiple synchronized quark and antiquark solid-state oscillators (colored and anticolor circles) coupled to generate frequencies for the $SU(2)$ gauged Bose-Einstein condensate with skyrmions²⁴ in the loop configuration based on the work of Afshari³⁷; the coupling circuits (gray triangles) shift the phase of the oscillators.

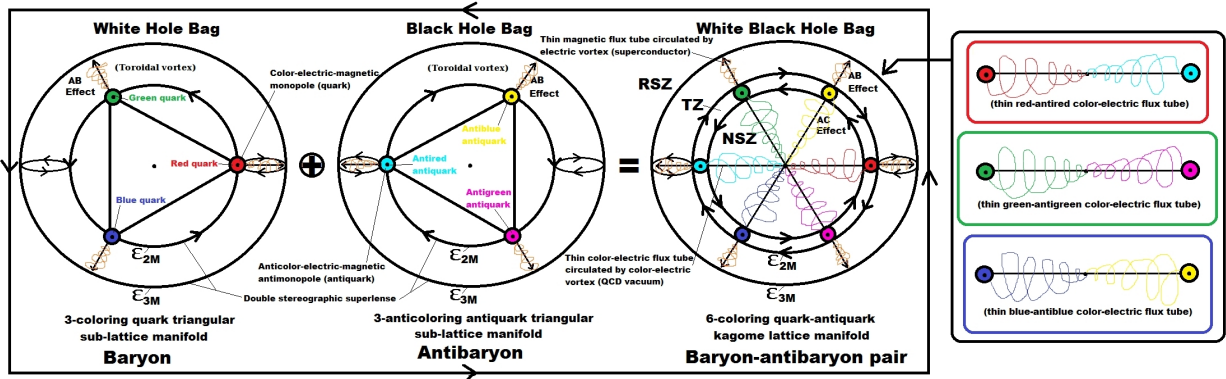


FIG. 3. The loop-induced zero-energy dynamics are described as “gluon dynamics”. The 3 distinct $q\bar{q}$ pairs for the WH-BH pair are “superbound” as coupled oscillators³⁷ to the Fermi surface in the upgraded Gribov vacuum generalized from³⁶ and are confined to the kagome lattice antiferromagnet on the six-coloring manifold. The $q\bar{q}$ pairs spontaneously generate *phase-excitations* (massless and pseudoscalar)^{6–9} and “Higgs-like” *amplitude-excitations* (massive and scalar)¹⁰ Laughlin excitations⁴. The toroidal vortex along the Riemannian holographic ring unit circle for a WH and/or BH is defined as a toroidal vortex between the spherical shells located at critical radius $\epsilon_{2M} = 2M$ and $\epsilon_{3M} = 3M$; double stereographic superlenses¹⁸ for two dynamical scales²². An affinity exists between WBHD and M.C. Escher’s duality, where the combined WH event horizon and BH event horizon at ϵ_{2M} exhibit the double horizon phenomena⁴⁷. The $q\bar{q}$ pairs confined to the TZ form thin color-electric flux tubes¹¹ in the QCD vacuum of the NSZ and exhibit the AC effect, while thin magnetic flux tubes in the RSZ superconductive region exhibit antiferromagnetic ordering and the AB effect; the QCD vacuum is to a superconductor, just as electricity is to magnetism, and just as the AC effect is to the AB effect. This model exhibits vortex-antivortex dancing⁴⁸ and confirms the spontaneous appearance of a stable 3D skyrmion in the $SU(2)$ gauged Bose-Einstein condensate of²⁴ confined to the Riemannian holographic ring unit circle on our 1D Riemann surface.

Laughlin’s fractional quantization¹² is axiomatic in this scenario. At proper temperature and pressure, the vacuum is consistent with Chernodub⁵³. Clearly, in treating the WBHD and superlensing dynamics, it is very convenient to separate the RSZ and NSZ degrees of freedom (Born–Oppenheimer approximation).

The NSZ and RSZ both represent *superconductive, FQHS 3-branes* interconnected by the TZ, which serves as a common (2D) surface boundary at ϵ_{2M} . The WH

and BH are spinning objects confined to the TZ so they generate whirlpools on both 3-brane distance scales in accordance with seashells closed on ϵ_{3M} ⁴⁶, thereby exhibiting the Magnus effect⁵⁴ and generating a vortex-antivortex dance⁴⁸; these whirlpools are described on the Riemann surface using spirals (i.e. weighted Fibonacci sequence and/or golden spiral). The TZ is a topological Mott insulator for^{25,49,55,56}, a Fermi surface as in⁵⁷, a Goldman–Laughlin quasiparticle interferometer of two

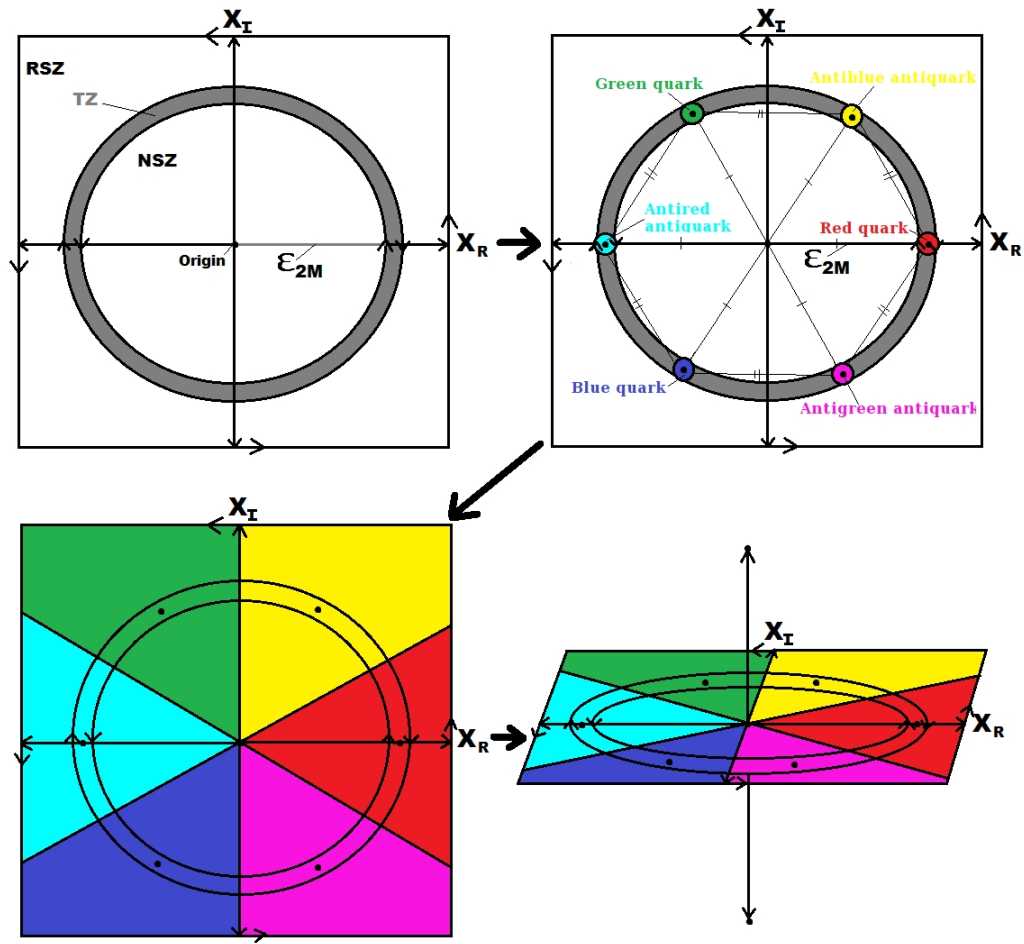


FIG. 4. The gauge-invariant TZ delineates the NSZ and RSZ: a 2-sphere which is dual to *both* 3-branes, where the $SU(2)$ Bose–Einstein condensate and gauge field is a 3D analogue of the Rashba spin-orbit coupling of the TZ, supporting the 1D, 2D, and 3D Skyrmion structures²⁴ (all). The WH-BH pair comprises the three distinct $q\bar{q}$ pairs and is modeled as a WBHB in the new Gribov vacuum with 18 quasiparticle signal zones (bottom).

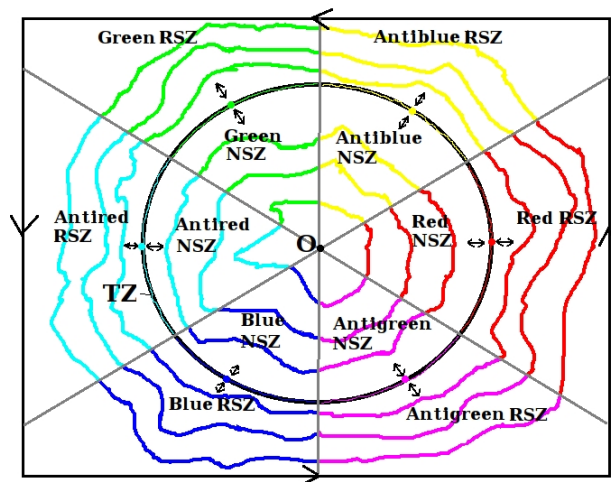


FIG. 5. The upgraded Gribov QCD/QED vacuum with 18 zones for quasiparticle signals pertaining to a WBHB on the 1D Riemann surface. The $q\bar{q}$ pairs are confined to the TZ, which is dual to the NSZ and the RSZ. The six-coloring spinon, holon, and orbion excitations are spontaneously generated and confined to the TZ, which acquires a geometric phase; the TZ excitations are dual to those of the NSZ and RSZ 3-branes.

counter-propagating edge channels as in⁵, a Gedanken interferometer as in⁵⁸, a quantum critical point as in^{4,59}, and a non-perturbative, self-consistent, $SU(2)$ gauged Bose-Einstein condensate as in⁶ that satisfies Novikov's self-consistency principle as in⁶⁰; a picture emerges of the vacuum as a conductor instead of "Dirac's insulator", with a new mass scale that reflects the position of the "Fermi surface"³⁶. The six-coloring antiferromagnetic alignment of the $q\bar{q}$ pairs spontaneously generate the physical behavior of the strong interaction as in⁴ and thereby triggers parity doubling, CPT violations, and different polarization rotation velocities on *both* the NSZ and RSZ distance scales simultaneously. Here, we identify the Dirac quantization and spin-charge magnetic monopole relations of⁶¹, Fermi liquid deviations of⁵⁹, non-linear optics, analogue gravity, and photon emissions analogous to the Hawking radiation as in⁶², and Andreev reflections of^{63,64}; the TZ's current continuously undergoes charge-transformation between the NSZ's and RSZ's supercurrent. The $q\bar{q}$ resonances form the exotic meson and broad locking states as in⁶⁵. The $q\bar{q}$ pairs and their waves are phase locked, spontaneously aligning to form dynamical 1D coherent accumulation structures with time-periodic flows¹³ and a von Kármán vortex street¹⁵ with impact parameters.

III. THE SPACE-TIME SURFACE AND GENERALIZED RIEMANN COORDINATES

Let X be the 1D Riemann surface. We define the complex number $x = x_{\mathbb{R}} + x_{\mathbb{I}}$ as a *position-point and position-vector* on X ; $x \in X$ is both a complex scalar and Euclidean vector with *amplitude* $|x|$ and *phase* $\langle x \rangle$, which are analogous to *magnitude* and *direction* in conventional notation. The orthogonal components of x , namely $x_{\mathbb{R}} \in \mathbb{R}^1$ and $x_{\mathbb{I}} \in \mathbb{I}^1$ as *axis-constrained* real and imaginary Euclidean vectors, respectively (where in this case \mathbb{I} denotes imaginary rather than irrational); the simple trichotomy axis-constraints for the \mathbb{R} -axis are

$$x_{\mathbb{R}} > 0 \Leftrightarrow \langle x_{\mathbb{R}} \rangle = 2\pi = 0, \quad (1)$$

$$x_{\mathbb{R}} = 0 \Leftrightarrow \langle x_{\mathbb{R}} \rangle = \frac{\pi}{2}, \quad (2)$$

$$x_{\mathbb{R}} < 0 \Leftrightarrow \langle x_{\mathbb{R}} \rangle = \pi, \quad (3)$$

and for the \mathbb{I} -axis are

$$x_{\mathbb{I}} > 0 \Leftrightarrow \langle x_{\mathbb{I}} \rangle = \frac{\pi}{2}, \quad (4)$$

$$x_{\mathbb{I}} = 0 \Leftrightarrow \langle x_{\mathbb{I}} \rangle = \frac{\pi}{4}, \quad (5)$$

$$x_{\mathbb{I}} < 0 \Leftrightarrow \langle x_{\mathbb{I}} \rangle = \frac{3\pi}{2}, \quad (6)$$

such that

$$|x_{\mathbb{R}}| = |x| \cos(\langle x \rangle), \quad (7)$$

$$|x_{\mathbb{I}}| = |x| \sin(\langle x \rangle), \quad (8)$$

with Pythagorean form

$$|x|^2 = x_{\mathbb{R}}^2 + x_{\mathbb{I}}^2, \quad \forall x \in X. \quad (9)$$

Thus, we've defined the 2D generalized (Riemann) coordinate system of X as

$${}^{2D}X : (x) = (x_{\mathbb{R}} + x_{\mathbb{I}}) = (x_{\mathbb{R}}, x_{\mathbb{I}}) = (|x|, \langle x \rangle), \quad \forall x \in X, \quad (10)$$

with respect to the unique reference origin-point $O \in X$, such that $(O) = (0 + 0i) = (0, 0i) = (0, 0\pi)$; $(x) = (x_{\mathbb{R}} + x_{\mathbb{I}})$ are 1D Riemann coordinates, $(x_{\mathbb{R}}, x_{\mathbb{I}})$ are 2D Cartesian coordinates, and $(|x|, \langle x \rangle)$ are Polar coordinates; a Complex-Cartesian-Polar synchronized and generalized coordinate system. The real and imaginary axis-constraints ensure that the generalized coordinates may always be expressed as a right-triangle with Pythagorean properties.

So how to we extend our 2D generalized coordinates of Definition (10) to 3D Schwarzschild space? Well, for a WH or BH of scale M (located precisely at the origin position-point $O \in X$) we define the 3D generalized (Schwarzschild) coordinate system of X as

$${}^{3D}X : (u_x, |x|, \langle x \rangle) = \left(\frac{M}{|x|}, |x|, \langle x \rangle \right), \quad \forall x \in X. \quad (11)$$

IV. ZONES

We define T as the TZ of X . So T is a topological representation of a Riemannian unit circle, where the critical radius of T is scaled and normalized to precisely $\epsilon_{2M} = 2M = \frac{\pi}{2}\epsilon_{scalar}$. We prove WBHC on T . ϵ_{scalar} is the *time unit scale-normalizing constant* and ϵ_{2M} is the inner confinement radius of T . Next, we define the circumference and wavelength of T , namely $T_{\lambda} = T_{circumference} = T_{wavelength} = 2\pi\epsilon_{scalar}$, as being equivalent to the (normalized) *Mikhail Grimov's area filling conjecture*⁶⁶: $T_{area} = T_{\lambda}$; $T \subset X$ is a closed curve and simple contour of surface position-points.

We use zone trichotomy to simultaneously define the TZ and SZ regions of X : we define X_- and X_+ as the NSZ and RSZ of X , respectively. The surface T delineates the topological sub-surfaces X_- and X_+ on X ; T is a Mott insulator²⁵ and Fermi surface³⁶ which delineates two dual superconductors^{25,49,55,56,63,64}. Thus, $\forall x \in X$ we know that precisely one of the following conditions must be satisfied:

$$|x| < \epsilon_{2M} \Leftrightarrow x \in X_-, \quad (12)$$

$$|x| = \epsilon_{2M} \Leftrightarrow x \in T, \quad (13)$$

$$|x| > \epsilon_{2M} \Leftrightarrow x \in X_+, \quad (14)$$

where clearly $X_- \cap T = T \cap X_+ = X_- \cap X_+ = \emptyset$ and $X_- \cup T \cup X_+ = X$. Hence, T is the multiplicative group of all non-zero complex 1-vectors, such that

$$T = \{t \in X : |t| = \epsilon_{2M}\}, \quad (15)$$

where we define all T position-points as *time-points* and

$$X_- = \{s \in X : |s| < \epsilon_{2M}\}, \quad (16)$$

$$X_+ = \{s \in X : |s| > \epsilon_{2M}\}, \quad (17)$$

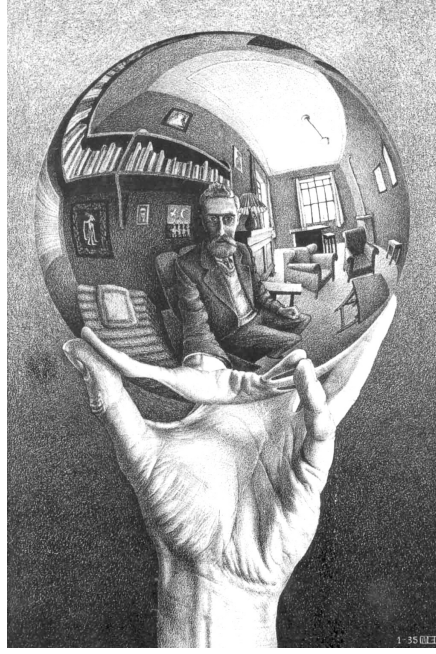


FIG. 6. The TZ is dual to *both* distance scales and imposes the double-confinement and double-lensing of M.C. Escher's duality⁴⁷; it is a stereographic superlense¹⁸ between the two 3-brane distance scales.

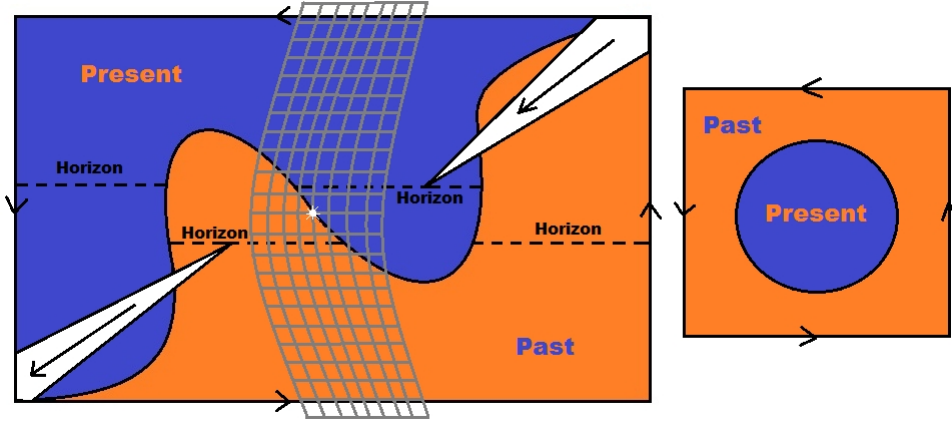


FIG. 7. Inopin's interpretation of M.C. Escher's double-horizons of⁴⁷ is directly connected to the $q \rightarrow \bar{q}$ transitions, past-present switching, time-reversal operation, and CPT-Theorem on the Riemann surface: time is circular and non-linear, so *the past is the future*. The quarks switch back and forth between the conjugate space-time regions with the appearance and disappearance of 3 quantum critical points in the QCD phase diagram.

where we define all $S = X_- \cup X_+$ position-points as *space-points*. So clearly,

$$\epsilon_{2M}^2 = |t|^2 = |t_{\mathbb{R}}|^2 + |t_{\mathbb{I}}|^2, \quad \forall t \in T, \quad (18)$$

$$|x|^2 = |x_{\mathbb{R}}|^2 + |x_{\mathbb{I}}|^2, \quad \forall x \in X. \quad (19)$$

So T is isometrically embedded in X with the one-to-one holographic mappings $f : T \hookrightarrow X$ and $f : T \rightarrow X_- \cup X_+$ with dual simultaneous bijections

$$f_{Time} : X_- \leftrightarrow T \hookrightarrow X_+, \quad (20)$$

$$f_{Space} : X_- \hookrightarrow T \leftrightarrow X_+, \quad (21)$$

for our dual space-time; we've proven that T is dual to X_- and T is also dual to X_+ . Interestingly, this formulation may provide a simplification to the Riemann-Hilbert problem as expressed in, for example,⁶⁷. Now because T is a type of Riemannian circle and holographic ring, we know it is a 2-sphere for the $SU(2)$ gauged Bose-Einstein condensate²⁴. Thus, for the position-point and position-vector $t \in T$ we apply Definition (10) to express the 2-sphere generalized and synchronized 2D Riemann coordinates

$${}^{2D}T : (t) = (t_{\mathbb{R}} + t_{\mathbb{I}}) = (t_{\mathbb{R}}, t_{\mathbb{I}}) = (|t|, \langle t \rangle) = (\epsilon, \langle t \rangle), \quad \forall t \in T, \quad (22)$$

and in 3D Schwarzschild coordinates

$${}^3D T : (u_t, |t|, \langle t \rangle) = \left(\frac{M}{|t|}, |t|, \langle t \rangle \right), \quad \forall t \in T. \quad (23)$$

Now because $\forall t \in T$ we have the uniform radius $|t| = \epsilon_{2M}$, we can alternatively drop the $|t|$ amplitude coordinate and just use the $\langle t \rangle$ phase coordinate to *directly* specify position-points on the 1D non-linear surface. Therefore, T is

- the 1D circular Abelian group $U(1)$;
- the 2D spherical non-Abelian group $SU(2)$; and
- isomorphic to the 3D orthogonal non-Abelian group $SO(3)$,

which directly supports 1D, 2D, and 3D skyrmions²⁴. So parity doubling²² is synonymous of the term degeneracy, and Escher gave an example of how one can establish 2D - 3D correspondence⁴⁷. We see here again the road to the t’Hooft and Maldacena holographic model for high-energy physics—all the 3D properties are inferred directly from the 2D (Riemannian holographic ring) domain⁶⁸.

We define T as a “fermiwire,” which is nothing more than a “nanowire”^{51,69} with Rashba spin-orbit coupling^{25,27,39} on the Fermi scale. The spin geometric phase for electrons in²⁷ is applied directly to the spin Hall effect³⁹, effective spin-dependent flux, and Andreev reflections^{63,64} of the quarks and antiquarks confined to the universal curve T (the holographic ring with uniform radius $|t| = \epsilon_{2M}$) embedded in X ; the duality derivation between the AAS effect and the AC effect of²⁷ is written for T as $\frac{\Phi_{mag}}{\Phi_0/2} \iff \sqrt{1 + \left(\frac{2m_t \langle t \rangle |t|}{\hbar^2} \right)^2}$, $\forall t \in T$, where Φ_{mag} is the magnetic flux, $\Phi_0 = h/e$ is the one flux quantum period, $\langle t \rangle = \alpha$ is the amplitude and strength of the Rashba spin-orbit interaction, and m_t is the effective mass; the left term is the AAS effect flux and the right term is the time-reversal AC effect oscillation unit with effective spin-dependent flux for the conductance modulation and voltage dependence observations of the AAS amplitude at zero magnetic field²⁷. This formulation is crucial to our six-coloring quark-antiquark configuration for the WBHC scenario because the magneto-resistance oscillations of^{27,70} along T are attributed to the AAS effect.

V. THE WAVEFUNCTION DEFINITION OF FRACTIONAL QUANTUM NUMBER ORDER PARAMETERS

Landau introduced the concept of OPs⁷¹, which we define as complex scalar fields⁶ on X . Here, we construct the WBWF using OPs and Laughlin statistics⁴ in our non-Abelian $SU(2)$ gauge theory. In the theory of superfluidity the OP measures the existence of Bose condensed

particles (Cooper pairs) and is given by the probability amplitude of such particles. The inter-particle forces between quarks and antiquarks, and between ⁴He and between ³He atoms, are *rotationally invariant in spin and orbital space* and, of course, conserve quantum number²². The latter symmetry gives rise to gauge symmetry, which is *broken* in any superfluid. First, for the theory of *isotropic* superfluids like a BCS superconductor or superfluid ⁴He, we define the *global* OP $\psi = \psi_{\mathbb{R}} + \psi_{\mathbb{I}}$ as a complex number (which inherits the notation similar to x as defined in Section III without loss of generality); ψ is both a complex scalar *and* Euclidean vector with the *amplitude* $|\psi|$ ¹⁰ and *phase* $\langle \psi \rangle$ components⁶. Then for *local* gauge SSB, we define the OP $\psi[x]$ as the complex scalar field

$$\psi[x] = \psi[x]_{\mathbb{R}} + \psi[x]_{\mathbb{I}}, \quad \forall x \in X, \quad (24)$$

where $|\psi[x]|$ and $\langle \psi[x] \rangle$ are the “gauge” amplitude and phase components local to $x \in X$, respectively, in accordance to Englert⁶. Furthermore, we define $\Delta|\psi[x]|$ and $\Delta\langle \psi[x] \rangle$ as the *change of* the OP’s amplitude and phase due to a “massive Higgs-like *amplitude-excitation*” and “massless Nambu-Goldstone *phase-excitation*” components, respectively—see Figures 8 and 9. Since the Mott insulator and stereographic superlense T is dual to both X_- and X_+ , we express Equation (24) specifically for time-points as the *parametric* function

$$\psi(t) = \psi(t)_{\mathbb{R}} + \psi(t)_{\mathbb{I}}, \quad \forall t \in T, \quad (25)$$

where the $SU(2)$ gauge-invariant T acquires a Berry–Aharonov–Anandan geometric phase as in⁵²; T is an *ordered medium* equipped with an OP space for topological defects. The classical energy density distribution along T is a function of the OP $\psi(t)$; within the ordered (superfluid) phase, Nambu-Goldstone and Higgs modes arise from the $\langle \psi(t) \rangle$ and $|\psi(t)|$, respectively, where the energy density transforms into a function for T with a minimum at $|\psi(t)| = 0$ ¹⁰. So $|\psi(t)|$ is excited with a periodic modulation of the spin-orbit coupling, which amounts to a “shaking” of the energy density (effective) potential for topological deformations along T in accordance with¹⁰. Furthermore, because the WH-BH pair is confined to T on the kagome lattice of antiferromagnetic ordering³⁸, we define the WBWF for the six-coloring position-points $\{r, g, b\} \subset T$ and $\{barr, \bar{g}, \bar{b}\} \subset T$ of three colored quarks and three anticolored antiquarks in the vacuum, respectively (recall Figures 3 and 4).

Above the critical temperature the system is invariant under an arbitrary change of the phase $\langle \psi[x] \rangle \rightarrow \langle \psi[x] \rangle'$, i.e. under a gauge transformation. Below the critical temperature a particular value of $\langle \psi \rangle$ is *spontaneously* preferred. In anisotropic superfluids, additional symmetries can be spontaneously broken, corresponding to *multiple* OP components of the WBWF. In ³He—the best studied example with multiple OP components—the pairs are in a spin-triplet state, meaning that rotational symmetry in spin space is broken, just as in a

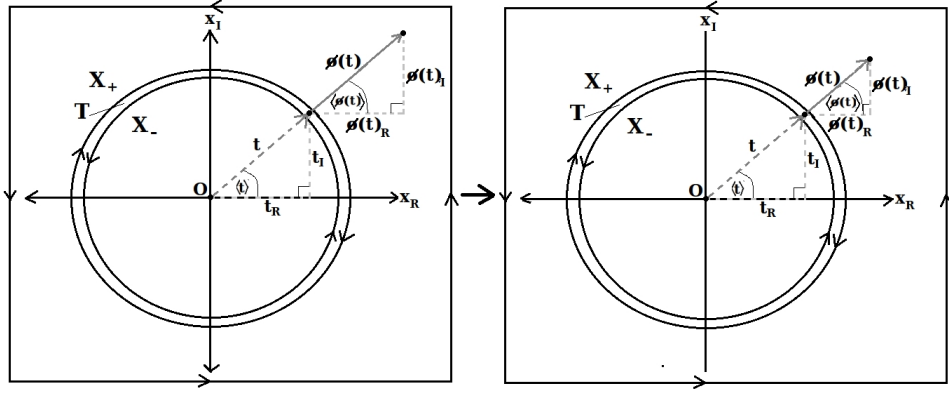


FIG. 8. A complex scalar field $\psi(t)$ experiences a massive “Higgs-like” *amplitude-excitation*¹⁰ (right), which is characteristic of the Nambu-Goldstone *scalar* boson SSB order parameter fluctuations discussed by⁶; a classical wave imposes volume effects and stretches the vacuum field.

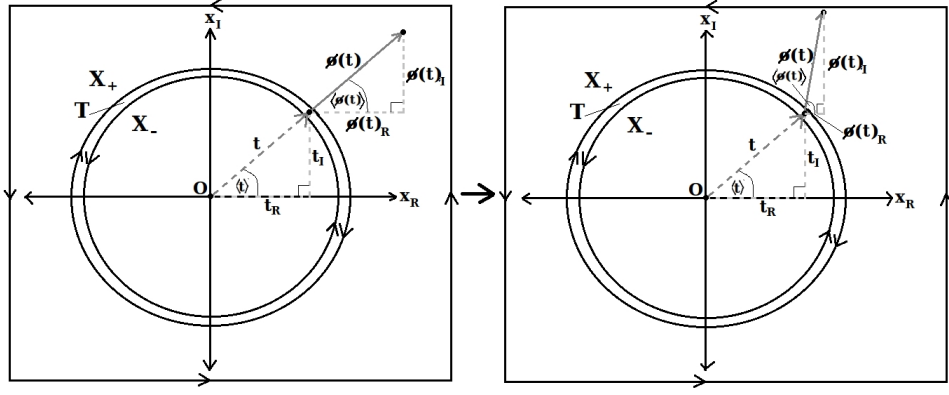


FIG. 9. A complex scalar field $\psi(t)$ experiences a *phase-excitation* (right), which is characteristic of the Nambu-Goldstone *pseudo-scalar* SSB order parameter fluctuations discussed by⁶; a classical wave imposes rotational effects on the vacuum field in accordance with vacuum degeneracy.

magnet. At the same time, the anisotropy of the Cooper-pair wavefunction in orbital space calls for a spontaneous breakdown of orbital rotation symmetry, as in *liquid crystals*²². Including the gauge symmetry, three symmetries are therefore broken in superfluid ^3He . The theoretical discovery that *several simultaneously broken symmetries* can appear in condensed matter was made by Antony Leggett, and represented a breakthrough in the theory of anisotropic superfluids, $^3\text{He}^{71}$. This leads to *superfluid phases* whose properties cannot be understood by simply adding the properties of systems in which each symmetry is *broken individually*. Such phases may have *long range* order in *combined*, rather than individual degrees of freedom. So to construct a strong WBWF constraint for WBHC to T , we “Cooper pair” the OP set of strongly conserved quantum numbers

$$\Phi_{OP} = \{\psi_C, \psi_I, \psi_J\}, \quad (26)$$

which is listed in Table I; the spin-orbit coupling of^{39,40,61} applies directly to T , where $\psi_J(t)$ is identical to the

“ B_{SO} -vector” of⁶⁹, such that

$$\psi_J(t) = \psi_S(t) + \psi_L(t), \quad \forall t \in T. \quad (27)$$

The $q\bar{q}$ pairs confined to T on the six-coloring kagome lattice manifold are located at position-points $r, g, b, \bar{r}, \bar{g}, \bar{c} \in T$; they adhere to the uniformly-arranged position-point constraints

$$\langle r \rangle = \langle \bar{r} \rangle \pm \pi, \quad \langle g \rangle = \langle \bar{g} \rangle \pm \pi, \quad \text{and} \quad \langle b \rangle = \langle \bar{b} \rangle \pm \pi, \quad (28)$$

with uniform amplitudes $|r| = |g| = |b| = |\bar{r}| = |\bar{g}| = |\bar{b}| = \epsilon_{2M}$, and antiferromagnetic ordering

$$\langle \psi_J(r) \rangle = \langle \psi_J(\bar{r}) \rangle \pm \pi, \quad (29)$$

$$\langle \psi_J(g) \rangle = \langle \psi_J(\bar{g}) \rangle \pm \pi, \quad \text{and} \quad (30)$$

$$\langle \psi_J(b) \rangle = \langle \psi_J(\bar{b}) \rangle \pm \pi, \quad (31)$$

(recall Figure 3). A little flight of imagination lead us to this new approach, where the OPs $\forall t \in T$ are “Cooper paired” to form a Leggett *superfluid B phase* of⁷¹ with azimuthal “alpha” phase angle $\langle t \rangle$; the OPs $\forall \psi \in \Phi_{OP}$ rotate freely in 2D and 3D space, while the superfluid

B phase angle $\langle t \rangle \in \{\langle r \rangle, \langle g \rangle, \langle b \rangle, \langle \bar{r} \rangle, \langle \bar{g} \rangle, \langle \bar{b} \rangle\}$ between them remains *constant*. Such phases form correlated helices along T , serving as constraints for the WBWF—see Figure 10.

Next, we construct our WBWF for the WBHB states. For a WH and BH centered on the origin-point $O \in X$ and confined to T we define the *full* baryon and antibaryon states as

$$\Psi_{total}(r, g, b) = \Psi(r) \times \Psi(g) \times \Psi(b) \quad \text{and} \quad (32)$$

$$\Psi_{total}(\bar{r}, \bar{g}, \bar{b}) = \Psi(\bar{r}) \times \Psi(\bar{g}) \times \Psi(\bar{b}), \quad (33)$$

respectively, for the WBHC and WBHD; the *red*, *green*, and *blue* quark wavefunctions respectively located at time-points $r, g, b \in T$ on the three-coloring triangular sub-lattice are

$$\Psi(r) = \psi_C(r) \times \psi_J(r) \times \psi_I(r) \times r, \quad \Psi(r) \stackrel{def}{=} \langle r | \Psi \rangle, \quad (34)$$

$$\Psi(g) = \psi_C(g) \times \psi_J(g) \times \psi_I(g) \times g, \quad \Psi(g) \stackrel{def}{=} \langle g | \Psi \rangle, \quad (35)$$

$$\Psi(b) = \psi_C(b) \times \psi_J(b) \times \psi_I(b) \times b, \quad \Psi(b) \stackrel{def}{=} \langle b | \Psi \rangle, \quad (36)$$

and the *antired*, *antigreen*, and *antiblue* antiquark wavefunctions respectively located at time-points $\bar{r}, \bar{g}, \bar{b} \in T$ on the three-anticoloring triangular sub-lattice are

$$\Psi(\bar{r}) = \psi_C(\bar{r}) \times \psi_J(\bar{r}) \times \psi_I(\bar{r}) \times \bar{r}, \quad \Psi(\bar{r}) \stackrel{def}{=} \langle \bar{r} | \Psi \rangle, \quad (37)$$

$$\Psi(\bar{g}) = \psi_C(\bar{g}) \times \psi_J(\bar{g}) \times \psi_I(\bar{g}) \times \bar{g}, \quad \Psi(\bar{g}) \stackrel{def}{=} \langle \bar{g} | \Psi \rangle, \quad (38)$$

$$\Psi(\bar{b}) = \psi_C(\bar{b}) \times \psi_J(\bar{b}) \times \psi_I(\bar{b}) \times \bar{b}, \quad \Psi(\bar{b}) \stackrel{def}{=} \langle \bar{b} | \Psi \rangle; \quad (39)$$

the WBWF for the three distinct $q\bar{q}$ pairs that are confined to T along the six-coloring kagome lattice manifold (recall Figure 3). So the antisymmetric WBWF is described with the six-coloring components

$$\Psi(r, \bar{r}) = -\Psi(\bar{r}, r), \quad (40)$$

$$\Psi(g, \bar{g}) = -\Psi(\bar{g}, g), \quad \text{and} \quad (41)$$

$$\Psi(b, \bar{b}) = -\Psi(\bar{b}, b), \quad (42)$$

for the confined quark and antiquark (two-particle) cases.

So for Definition (32) and the related six-coloring Definitions (31–37), we define the full WBWF antisymmetrization via the covariant antisymmetric metric tensor: the 2D antisymmetric WBWF matrix

$$\begin{pmatrix} 0 & \Psi_{total}(r, g, b) \\ \Psi_{total}(\bar{r}, \bar{g}, \bar{b}) & 0 \end{pmatrix} \quad (43)$$

and the expanded 3D antisymmetric WBWF matrix

$$\begin{pmatrix} 0 & \Psi(r) & \Psi(g) \\ \Psi(\bar{r}) & 0 & \Psi(b) \\ \Psi(\bar{g}) & \Psi(\bar{b}) & 0 \end{pmatrix} \quad (44)$$

for T . So given complex tangent vectors μ and ν we define

$$g_x(\mu, \nu) = -g_x(\nu, \mu) \in \mathbb{C}, \quad \forall x \in X; \quad (45)$$

the tensor describes the X curvature (“vector phase”) $\langle g_x(\mu, \nu) \rangle$ and the field strength (“vector amplitude”) $|g_x(\mu, \nu)|$ at a position-point $x \in X$. The Levi-Civita symbol for the color singlet function is

$$\zeta_{rgb} = \zeta^{rgb} = \begin{cases} +1 & \text{if } (r, g, b) \text{ is } (1, 2, 3), (2, 3, 1), \text{ or } (3, 1, 2) \\ 0 & \text{if } r = g \text{ or } g = b \text{ or } b = r \\ -1 & \text{if } (r, g, b) \text{ is } (3, 2, 1), (2, 1, 3), \text{ or } (1, 3, 2) \end{cases} \quad (46)$$

The CPT-Theorem is a fundamental property of T . Hence, for a WH or BH of scale M we have the OP charge transformation(s), $\forall \psi \in \Phi_{OP}$,

$$C : \begin{cases} \psi(t) & \mapsto -\psi(t), \\ \begin{pmatrix} \psi(t)_{\mathbb{R}} \\ \psi(t)_{\mathbb{I}} \end{pmatrix} & \mapsto \begin{pmatrix} -\psi(t)_{\mathbb{R}} \\ -\psi(t)_{\mathbb{I}} \end{pmatrix}, \\ \begin{pmatrix} |\psi(t)| \\ \langle \psi(t) \rangle \end{pmatrix} & \mapsto \begin{pmatrix} |\psi(t)| \\ \langle \psi(t) \rangle \pm \pi \end{pmatrix}, \end{cases} \quad (47)$$

the *parity transformation*(s) (in generalized 2D Riemann coordinates for 3D Schwarzschild space) is the flip in the sign of the one coordinate

$$P : \begin{cases} \begin{pmatrix} t_{\mathbb{R}} \\ t_{\mathbb{I}} \\ \frac{M}{|t|} \end{pmatrix} & \mapsto \begin{pmatrix} -t_{\mathbb{R}} \\ -t_{\mathbb{I}} \\ -\frac{M}{|t|} \end{pmatrix}, \\ \begin{pmatrix} |t| \\ \langle t \rangle \\ \frac{M}{|t|} \end{pmatrix} & \mapsto \begin{pmatrix} |t| \\ \langle t \rangle \pm \pi \\ -\frac{M}{|t|} \end{pmatrix}, \end{cases} \quad (48)$$

and *time reversal transformation*(s)

$$T : \begin{cases} t & \mapsto -t, \\ \begin{pmatrix} t_{\mathbb{R}} \\ t_{\mathbb{I}} \end{pmatrix} & \mapsto \begin{pmatrix} -t_{\mathbb{R}} \\ -t_{\mathbb{I}} \end{pmatrix}, \\ \begin{pmatrix} |t| \\ \langle t \rangle \end{pmatrix} & \mapsto \begin{pmatrix} |t| \\ \langle t \rangle \pm \pi \end{pmatrix}, \end{cases} \quad (49)$$

which comprise a CPT-transformation, $\forall t \in T$. We see that for Definitions (47), (48), and (49) there are multiple equivalent transformations for each case because the generalized Riemann coordinates of Definition (10) and the OP Definition (24) use synchronized Complex-Cartesian-Polar values (where the magnitude and direction of the Polar components are replaced with amplitude and phase, respectively).

VI. THE LAGRANGIAN: EFFECTIVE POTENTIAL AND EFFECTIVE KINETIC

Here, we express the gauged SSB in our FQHS space-time scenario on X , which is applicable to both 2D and

TABLE I. The quantum number order parameters for the WBWF states on the 1D Riemann surface X . Here, $\psi_J = \psi_S + \psi_L$ and $\psi_J(t) = \psi_S(t) + \psi_L(t)$ for the spin-orbit coupling of the holographic confinement ring $T \subset X$.

Order Parameter	Symbol	Global	Local
Color Charge	C	$\psi_C = \psi_{C_{\mathbb{R}}} + \psi_{C_{\mathbb{I}}}$	$\psi_C[x] = \psi_C[x]_{\mathbb{R}} + \psi_C[x]_{\mathbb{I}}$
Isospin	I	$\psi_I = \psi_{I_{\mathbb{R}}} + \psi_{I_{\mathbb{I}}}$	$\psi_I[x] = \psi_I[x]_{\mathbb{R}} + \psi_I[x]_{\mathbb{I}}$
Orbital Angular Momentum	L	$\psi_L = \psi_{L_{\mathbb{R}}} + \psi_{L_{\mathbb{I}}}$	$\psi_L[x] = \psi_L[x]_{\mathbb{R}} + \psi_L[x]_{\mathbb{I}}$
Spin Angular Momentum	S	$\psi_S = \psi_{S_{\mathbb{R}}} + \psi_{S_{\mathbb{I}}}$	$\psi_S[x] = \psi_S[x]_{\mathbb{R}} + \psi_S[x]_{\mathbb{I}}$
Total Angular Momentum	J	$\psi_J = \psi_{J_{\mathbb{R}}} + \psi_{J_{\mathbb{I}}}$	$\psi_J[x] = \psi_J[x]_{\mathbb{R}} + \psi_J[x]_{\mathbb{I}}$

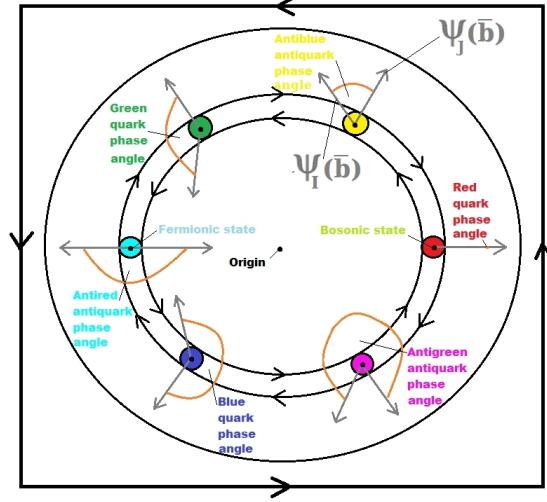


FIG. 10. Leggett's⁷¹ six distinct superfluid B phase angles for the three $q\bar{q}$ pairs confined to T along the six-coloring kagome lattice of antiferromagnetic ordering^{4,38}. The superfluid B phase angles $\langle r \rangle, \langle g \rangle, \langle b \rangle, \langle \bar{r} \rangle, \langle \bar{g} \rangle, \langle \bar{b} \rangle$ remain *constant* and correlate the OPs as they rotate freely in 2D and 3D space; this *long range order* applies $\forall t \in T, \forall \psi \in \Phi_{OP}$, to form correlated helices along T ; this concept serves as a strong WBWF constraint and applies to all OPs for a given time-point. In this diagram, only $\psi_J(t)$ and $\psi_I(t)$ are shown, but $\psi_C(t)$ is also correlated with $\langle t \rangle$.

3D space; the Lagrangian is defined as

$$\mathcal{L}[x] = E_K[x] - E_P[x], \quad \forall x \in X, \quad (50)$$

using our generalized coordinates, where $E_K[x]$ and $E_P[x]$ are the *effective kinetic* and *effective potential*, respectively, for a position-point x . From⁷² the gauge boson's E_P is defined as

$$E_P[x] = \frac{\sqrt{1-2u_x}}{|x|}, \quad \forall x \in X. \quad (51)$$

The E_P depends on the Schwarzschild geometry but not on the choice of orbit. Only one E_P is required to analyze the motion of all radiation (including radio waves, radar pulses, gamma rays, etc.). It is important to stress E_P differences and similarities between a massive particle and its massless limit: radiation-rays. Next, the E_K is defined as

$$E_K[x] = \frac{1}{2}m_x v_x^2 = \frac{1}{2} \frac{F_x}{a_x} v_x^2, \quad \forall x \in X, \quad (52)$$

where F_x is the *effective force*, where m_x is the *effective mass*, a_x is the *effective acceleration*, and v_x is the *effective velocity* of the particle at x in the FQHS space-time.

Einstein's F_x , the E_P *per unit of particle effective mass* m_x , is defined as

$$F_x = m_x a_x = \frac{E_P[x]}{m_x} = \sqrt{(1-2u_x) \left[1 + \frac{(\frac{J}{m_x})^2}{|x|^2} \right]}, \quad \forall x \in X, \quad (53)$$

where the a_x along coordinate phase $\langle x \rangle$ is

$$a_x = \frac{1}{\hbar^2} \sum_{m_x} \frac{\partial^2 \varepsilon(k_x)}{\partial k_{\langle x \rangle} \partial k_{m_x}} e_x E_{m_x}, \quad \forall x \in X, \quad (54)$$

where k_x is the wave vector, $\varepsilon(k_x)$ is the dispersion relation, and e_x is the point charge in an external electric field E .

VII. CONCLUSION AND OUTLOOK

In this first paper of the series, we introduced the topologies, vacuum, 2D and 3D generalized coordinates, fractional statistics, WBWF quantum number OPs, gauge symmetry breaking, and Lagrangian for our WBHC proof and WBHD in FQHS space-time. In the

next paper(s) of this series, we will extend our quark-antiquark confinement scenario by discussing the anyons, phase locking, HH, attractive and repulsive gravitational effects of quasiparticle signals on the Lagrangian, modified Gullstrand–Painlevé reference frames, and Magnification Effect.

In our opinion, this proof of quark-antiquark confinement with the amplitude–excitations and phase–excitations begins to reveal additional fundamental mechanisms and relationships inherent to our universe. In doing so, we’ve been able to shed more light on a

number of mysterious concepts in nature, including BHs, WHs, baryon asymmetry, creation, annihilation, double horizons, and FQHS space-time. We suspect that these formulations, which are inspired by a plethora of experimental data, can be used to construct a unified field theory in the near future, thereby advancing physics to the “next level.” Through global cooperation, competition, hard work, and creativity, these powerful concepts can be further scrutinized, extended, and applied to virtually all areas of mathematics, science, medicine, and engineering.

* inopinandrej@yahoo.com

† nathanschmidt@u.boisestate.edu

- 1 K. Thome, *Black Holes and Time Warps: Einstein’s outrageous legacy* (New York: WW Norton&Company, 1994)
- 2 S. Carroll, *Spacetime and geometry. An introduction to general relativity*, vol. 1 (2004)
- 3 J. Shu, *Connecting LHC signals with deep physics at the TeV scale and baryogenesis* (ProQuest, 2008)
- 4 R. Laughlin, Arxiv preprint cond-mat/9802180 (1998)
- 5 F. Camino, W. Zhou, V. Goldman, *Physical Review B* **72**(7), 075342 (2005)
- 6 F. Englert, Arxiv preprint hep-th/1204.5382v1 (2012)
- 7 J. Goldstone, Selected papers of Abdus Salam:(with commentary) **5**, 204 (1994)
- 8 Y. Nambu, *Physical Review Letters* **4**(7), 380 (1960)
- 9 Y. Nambu, G. Jona-Lasinio, *Physical Review* **122**(1), 345 (1961)
- 10 M. Endres, T. Fukuhara, D. Pekker, M. Cheneau, P. Schauß, C. Gross, E. Demler, S. Kuhr, I. Bloch, *Nature* **487**(7408), 454 (2012)
- 11 E. Witten, *Current Science-Bangalore-* **81**(12), 1576 (2001)
- 12 R. Laughlin, Nobel lectures, physics, 1996-2000 p. 264 (2002)
- 13 D. Pushkin, D. Melnikov, V. Shevtsova, *Physical Review Letters* **106**(23), 234501 (2011)
- 14 Q. Hu, Arxiv preprint physics/0512265 (2005)
- 15 M.J. Thoraval, K. Takehara, T.G. Etoh, e.a. Popinet, Stéphane, *Phys. Rev. Lett.* **108**, 264506 (2012). doi: 10.1103/PhysRevLett.108.264506
- 16 R. Shelby, D. Smith, S. Nemat-Nasser, S. Schultz, *Applied Physics Letters* **78**, 489 (2001)
- 17 J. Li, C. Chan, *Physical Review E* **70**(5), 055602 (2004)
- 18 U. Leonhardt, *New Journal of Physics* **11**, 093040 (2009)
- 19 V. Veselago, E. Narimanov, *Nature materials* **5**(10), 759 (2006)
- 20 W. Melnitchouk, R. Ent, C. Keppel, *Physics reports* **406**(3), 127 (2005)
- 21 B. Kopeliovich, B. Povh, I. Schmidt, arXiv:hep-ph/0607337v1 [hep-ph] (2006)
- 22 A. Inopin, in *AIP Conference Proceedings*, vol. 1030 (2008), vol. 1030, p. 298
- 23 P. Zhang, P. Horvathy, J. Rawnsley, *Annals of Physics* **327**, 118 (2012)
- 24 T. Kawakami, T. Mizushima, M. Nitta, K. Machida, *Phys. Rev. Lett.* **109**, 015301 (2012). doi: 10.1103/PhysRevLett.109.015301. URL <http://link.aps.org/doi/10.1103/PhysRevLett.109.015301>
- 25 J. Schlappa, K. K. Wohlfeld, M.e.a. Zhou J., Mourigal, *Nature* (2012)
- 26 Y. Aharonov, J. Anandan, *Physical Review Letters* **58**(16), 1593 (1987)
- 27 F. Nagasawa, J. Takagi, Y. Kunihashi, e.a. Kohda, *Physical Review Letters* **108**(12), 086801 (2012)
- 28 K. Richter, *Physics* **5**, 22 (2012). doi:10.1103/Physics.5.22. URL <http://link.aps.org/doi/10.1103/Physics.5.22>
- 29 M. Olsson, arXiv:hep-ph/0001227 (2000)
- 30 S. Todorova, Arxiv preprint arXiv:1101.2407 (2011)
- 31 S. Todorova, arXiv:1204.2655v1 [hep-ph] (2012)
- 32 P. Cortet, A. Chiffaudel, F. Daviaud, B. Dubrulle, *Physical review letters* **105**(21), 214501 (2010)
- 33 C. Varney, K. Sun, V. Galitski, M. Rigol, *Physical Review Letters* **107**(7), 77201 (2011)
- 34 D. Siegel, C. Park, C. Hwang, e.a. Deslippe, J., *Proceedings of the National Academy of Sciences* **108**(28), 11365 (2011)
- 35 A. Paramekanti, L. Balents, M. Fisher, Arxiv preprint cond-mat/0203171 (2002)
- 36 F. Close, Y. Dokshitzer, V. Gribov, e.a. Khoze, V.A., *Physics Letters B* **319**(1), 291 (1993)
- 37 Y. Tousi, V. Pourahmad, E. Afshari, *Physical Review Letters* **108**(23), 234101 (2012)
- 38 O. Cépas, A. Ralko, *Physical Review B* **84**(2), 020413 (2011)
- 39 S. Souma, B. Nikolić, *Physical review letters* **94**(10), 106602 (2005)
- 40 T. Chen, G. Guo, *Physical Review B* **79**(12), 125301 (2009)
- 41 C. Pappas, *Physics* **5**, 28 (2012). doi:10.1103/Physics.5.28. URL <http://link.aps.org/doi/10.1103/Physics.5.28>
- 42 K. Marty, V. Simonet, E. Ressouche, e.a. Ballou, R., Arxiv preprint arXiv:0809.3067 (2008)
- 43 E. Edlund, O. Lindgren, M.N. Jacobi, *Phys. Rev. Lett.* **108**, 165502 (2012). doi:10.1103/PhysRevLett.108.165502. URL <http://link.aps.org/doi/10.1103/PhysRevLett.108.165502>
- 44 A. Bostwick, F. Speck, T. Seyller, e.a. Horn, K., *Science* **328**(5981), 999 (2010)
- 45 A. Principi, R. Asgari, M. Polini, *Solid State Communications* (2011)
- 46 A. Inopin, arXiv:hep-ph/0702257v1 [hep-ph] (2007)
- 47 M. Escher, B. Ernst, J. Brigham, *The magic mirror of MC Escher* (Random House, 2007)
- 48 P. Engels, *Physics* **3**, 33 (2010)
- 49 D. Sticlet, C. Bena, P. Simon, *Physical Review Letters* **108**(9), 096802 (2012)

- ⁵⁰ C. Quay, T. Hughes, J. Sulpizio, L.e.a. Pfeiffer, *Nature Physics* **6**(5), 336 (2010)
- ⁵¹ S. Nadj-Perge, V. Pribiag, J. Berg, e.a. Zuo, *Physical Review Letters* (2012)
- ⁵² P. Bruno, *Phys. Rev. Lett* **108**, 240402 (2012)
- ⁵³ M. Chernodub, *Physical Review D* **82**(8), 085011 (2010)
- ⁵⁴ E. Sonin, *Physical Review B* **55**(1), 485 (1997)
- ⁵⁵ L. Fu, C. Kane, *Physical review letters* **100**(9), 96407 (2008)
- ⁵⁶ J. Sau, R. Lutchyn, S. Tewari, S. Das Sarma, *Physical review letters* **104**(4), 40502 (2010)
- ⁵⁷ V.N. Gribov, *Eur. Phys. J. C* 10 pp. 91–105 (1999)
- ⁵⁸ V. Jacques, F. Grosshans, F. Treussart, P. Grangier, *Science Magazine* **315**(5814), 966 (2007)
- ⁵⁹ H. Pfau, S. Hartmann, U. Stockert, e.a. Sun, P., *Nature* **484**(7395), 493 (2012)
- ⁶⁰ J. Friedman, M. Morris, I. Novikov, F.e.a. Echeverria, *Physical Review D* **42**(6), 1915 (1990)
- ⁶¹ F. Wilczek, *Physical Review Letters* **48**(17), 1144 (1982)
- ⁶² D. Faccio, (2011)
- ⁶³ X. Du, I. Skachko, E. Andrei, *Physical Review B* **77**(18), 184507 (2008)
- ⁶⁴ H. Nilsson, P. Samuelsson, P. Caroff, H. Xu, *Nano Letters* (2012)
- ⁶⁵ V. Anisovich, D. Bugg, A. Sarantsev, *Physical Review D* **58**(11), 111503 (1998)
- ⁶⁶ V. Bangert, C. Croke, S. Ivanov, M. Katz, *Geometric and Functional Analysis* **15**(3), 577 (2005)
- ⁶⁷ A. Its, *Notices of the AMS* **50**(11), 1389 (2003)
- ⁶⁸ J. Maldacena, *Scientific American* **11**, 57 (2005)
- ⁶⁹ V. Mourik, K. Zuo, S. Frolov, e.a. Plissard, SR, *Arxiv preprint arXiv:1204.2792* (2012)
- ⁷⁰ B. Pannetier, J. Chaussy, R. Rammal, P. Gandit, *Phys. Rev. B* **31**, 3209 (1985). doi:10.1103/PhysRevB.31.3209. URL <http://link.aps.org/doi/10.1103/PhysRevB.31.3209>
- ⁷¹ A. Reading, *Rev. Mod. Phys* **47**, 331 (1975)
- ⁷² E. Taylor, J. Wheeler, *Recherche* **67**, 02 (2000)